Improving the sensitivity and the cost-effectiveness of a competitive visual lateral flow immunoassay through sequential designs of experiments

Improving the sensitivity and the cost-effectiveness of a competitive visual lateral flow immunoassay through sequential designs of experiments

Simone Cavalera, [a] Alessandro Gelli,[a] Fabio Di Nardo,[a] Thea Serra,[a] Valentina Testa,[a] Stefano Bertinetti,[a] Laura Ozella,[b] Claudio Forte,[b] Claudio Baggiani,[a] and Laura Anfossi.[a]

a. Department of Chemistry, University of Turin, Turin (TO), Italy
b. Department of Veterinary Sciences, University of Turin, Grugliasco (TO), Italy

ORCIDS

- Simone Cavalera 0000-0002-5353-647X
- Alessandro Gelli 0009-0006-9944-0867
- Fabio Di Nardo 0000-0003-0497-4251
- Thea Serra 0000-0001-9271-5174
- Valentina Testa 0000-0002-8976-9160
- Stefano Bertinetti 0000-0003-1982-247X
- Laura Ozella 0000-0001-7371-3309
- Claudio Forte 0000-0002-0060-3851
- Claudio Baggiani 0000-0003-1024-2532
- Laura Anfossi 0000-0002-2920-0140

Corresponding author: Simone Cavalera
Department of Chemistry, University of Turin, via Pietro Giuria 7, Turin (TO), Italy
e-mail: simone.cavalera@unito.it

Abstract

Although visual lateral flow immunoassays (LFIAs) are advantageous analytical tools, they typically suffer from low sensitivity in the competitive format (cLFIA). Optimizing sensitivity in this format is challenging as it depends on the inhibition of a visual signal. To optimize the sensitivity of a cLFIA, an experimental design-based approach is proposed and illustrated for the detection of cortisol. Gold nanoparticles (AuNPs) are used to label monoclonal anti-cortisol antibodies (Ab) to generate the probe. The Ab:AuNP ratio, the amount of probe and competitor on the test line are proposed as relevant parameters for optimization. As discriminatory conditions for sensitivity, the simultaneous disappearance of the color in the presence of a certain level of cortisol and a clearly visible color in its absence were assumed. A decision process called 4S (start, shift, sharpen, stop) is proposed for the interpretation of the response surfaces obtained after multivariate modelling of the data set. Using this approach, sensitivity was improved >500-fold (visual LOD =20.5±1.0 ng/mL, LOD=0.28 ng/mL) after 13 experiments and 10-fold (vLOD=2.2±0.1 ng/mL, LOD=0.07 ng/mL) after 21 additional experiments. Reagent consumption was simultaneously reduced 40-fold. The feasibility of cortisol detection in human saliva samples was established with a satisfactory recovery of 70-109%. The strategy from this work is useful for designing highly sensitive cLFIAs by unravelling the full potential of the immunoreagents and labels employed, with a limited number of experiments and reagent consumption, and without sacrificing the simplicity and affordability of visual, stand-alone LFIAs.

Keywords: Point-of-care testing, Rapid test, Immunosensor, Gold Nanoparticles, Cortisol, Immunochromatographic assay, visual LOD

Since its first appearance, in 1956, the Lateral Flow Immunoassay (LFIA) has progressively gained the attention of analyst [1,2]. Today, it is a well-established and world-widely diffused technique, employed for many applications, including, but not limited to, clinical[3–5], veterinary, toxicological[6,7] and food safety[8,9] fields. The LFIA relies on the specificity of the antibody-antigen binding [10], similarly to the Enzyme Linked Immunosorbent Assay (ELISA)[11]; however, it enables the realization of the assay outside the laboratory and at the point-of-care. A simplified schematic of a LFIA device **(Figure 1a)** includes a porous membrane through which the liquid sample flows by capillarity, some specific bioreagents (i.e. antibodies and antigens), which are immobilized onto the membrane, perpendicularly to the flow, to form specific reactive zones, and a labelled bioreagent (again an antigen or an antibody), which interacts with the analyte in the sample and with the reactive zones. The binding of the labelled bioreagent to the reactive zones is revealed by detecting the signal of the label.

Although different detection strategies and various labelling materials have been proposed to be used in the LFIA platform, the colorimetric detection based on the visual read-out of results is the most diffused format both in the literature and, especially, on the market. The reasons behind the popularity of visual LFIAs, especially the ones including gold nanoparticles (AuNP) as the labels, are numerous (i.e.: cost-effectiveness, robustness, simplicity in use and interpretation, portability, etc…) and are summarized by the ASSURED (affordable, sensitive, specific, user-friendly, rapid, equipment-free, delivered) criteria established by the World Health Organization[12]. Despite several advantages, the most widely recognized drawback of colorimetric (visual) LFIA is the poor sensitivity[13,14]. Nevertheless, among the colorimetric probes (such as latex encapsulating dyes, colored microparticles, and metal nanoparticles) the plasmonic materials, and AuNPs above all, provide a way more intense detectability[15–17]. This is due to the unique features of the material itself, which led them to be the most employed probe in visual-readout LFIA[9].

To address this limitation though preserving advantages connected to the visual read-out, various colored nanomaterials were proposed, including large AuNPs [18], composite nanomaterials [19], and carbon-based nanomaterials [20] Some authors introduced some enhancing steps, which followed the antigen-antibody reaction to increase the overall signal (such as, for example, the addition of other gold nanoparticles[21], the deposition of a second layer of gold formed locally by the reduction of gold ions[22] or others approaches [9,13,23–25]. If the colorimetric LFIA is made without the gold nanoparticles, using an alternative label instead, this is generally optimized for its own synthetic characteristics and involvement within the assay[26–31]. These methods enabled significant improvement in terms of sensitivity, however complicating the use of the devices and reducing their practical applications. Additionally, guidelines for designing and optimizing LFIA devices and especially to maximize the sensitivity have been reported for non-competitive LFIA [32].

The optimization of the sensitivity of LFIAs has been approached in several ways over the years. When the topic was not related to gold-based colorimetric LFIA but the employment of a new label, strategy, or detection technique the optimization focused on the particular variables of the new material[33–35],

technology [36,37] or experimental conditions in general[38–41]. In these cases, comparisons with gold-based colorimetric LFIA were made but this latter was generally not optimized. When the optimization was conducted on a colorimetric LFIA, it regarded the device materials (such as the membrane, the conjugate and sample pads) [42,43]. Colorimetric LFIA based on gold nanoparticles have been optimized, especially for challenging applications in terms of sensitivity (e.g: mycotoxins detection)[44–46]. Among these papers, the ones involving a competitive format applied various strategies. Some of them measured the signal in the absence of the analyte and at one concentration point [44], few points[26,47] or built the whole calibration curve[27,45,46]. These approaches were functional to reach high sensitivity, but many experiments were needed, and the reagents consumption was remarkable after the whole optimization process. Most important, all these optimization works have been carried out by using a sequential approach and there are very few examples of the employment of a multivariate approach for such purpose.

For competitive LFIA, the format needed for detecting small molecules, the "less is more" rule has been suggested to increase the sensitivity, that is the less the antibody used in the assay, the higher the sensitivity reached. [23] In immunoassay theory, competitive assays require the use of a limited amount of antibody [48]. This is because there is competition between the analyte and the competitor (labelled or anchored analyte derivative) for binding to a limited number of antibody sites. The signal is provided by the antibody-competitor complex and is inversely related to the amount of analyte. The sensitivity of the assay is then determined by the ability of the analyte to inhibit antibody-competitor complex formation to a measurable extent. The lower the amount of antibody, the lower the amount of analyte required to occupy antibody sites and reduce the sites available for binding to the competitor. Reducing the amount of competitor also favours the analyte in the competition. However, the amount of competitor must be sufficient to give an intense signal in the absence of the analyte, otherwise no decrease in the signal itself will be observed in the presence of the analyte. This is a general rule for all competitive immunoassays, regardless of the platform used (ELISA, CLIA, biosensors, etc.), but it is particularly true for LFIA, where the immunoreactions take place in a flow and there is no time for equilibration[23]. Other parameters, particularly affinity, affect the optimal concentration of antibody, so the amount to be used must be optimised for each particular antibody. The achievement of high sensitivity is especially challenging when competitive assays are realized[18,49]. Moreover, the definition of the limit of detection for visual LFIAs complicates it further. In fact, the visual limit of detection (vLOD) of a colorimetric LFIA is defined as the concentration of the analyte that provides the appearance/disappearance of the signal at the analyte-responsive reactive line, thus providing a simple yes/no interpretation. In non-competitive LFIAs, the vLOD reflects the minimum detectable amount of the analyte (vLOD=LOD), while for competitive LFIAs the vLOD corresponds to the complete inhibition of the binding of the labelled antibody to the antigen, which usually occurs at the upper limit of quantification of the assay (**Figure 1b**).

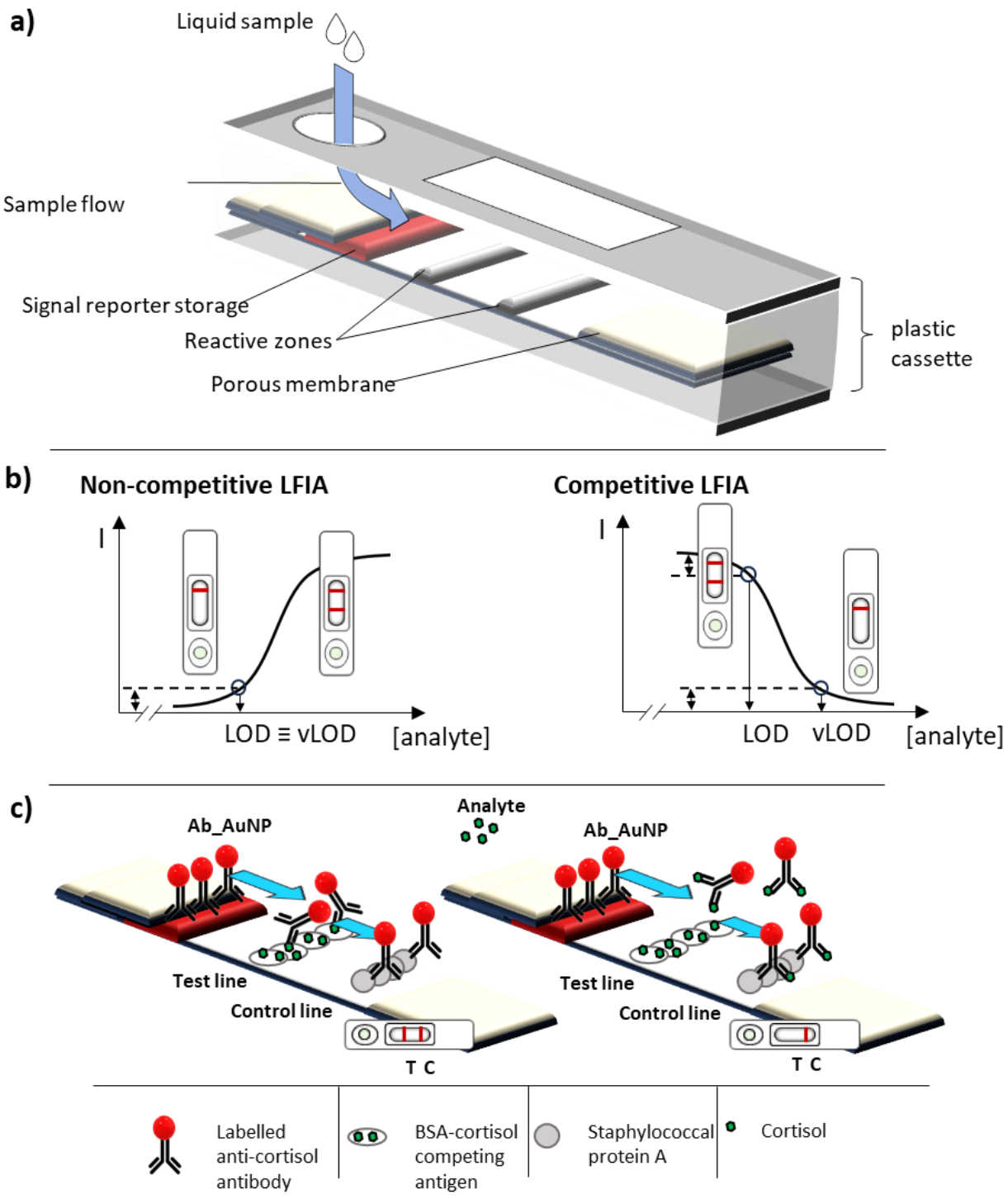

Figure 1: Schematic of: (a) the working principle of the lateral flow device; (b) the analytical signal for non-competitive and competitive LFIAs and the correspondence with the visual output; (c) the competititve LFIA for cortisol detection developed and optimized in this work.

The LFIA development rarely includes a systematic unbiased optimization of the experimental conditions to maximize the sensitivity because of the large number of experiments required and the consume of (expensive and finite) reagents. Nonetheless, by means of an appropriate approach based on experimental design, the number of experiments can be restricted[50–52]. Recently, we evaluated the application of the experimental

design for the optimization of a non-competitive LFIA for the simultaneous detection of two strains of the bovine Foot-and-Mouth Disease Virus[53]. The approach was then employed in other non-competitive LFIAs showing significant improvement of the sensitivity [54,55].

Here, we proposed a general strategy based on the use of the experimental design (DoE) with the aim of guiding the development of high-sensitive visual LFIAs in the competitive format, which may be employed for the detection of several classes of relevant (bio)markers, such as hormones[56], drugs[57], toxins[58,59], etc... The strategy was resumed in four actions, named Start, Shift, Sharpen, and Stop (4S) (**Figure 2**). The idea underlying the 4S process was the execution and the elaboration of sequential DoE, up to achieving the maximal (or required) sensitivity. The 4S process included a first DoE designed for the exploration of the variables into a 'rational' interval (Start); after the elaboration, the operator decided whether: i) not proceeding (Stop), because the satisfying sensitivity was reached; or ii) proceeding with a second exploration in a different intervals of the variables (Shift), in case of insufficient sensitivity); or iii) zooming in a narrower interval and tightening the criteria (Sharpen), in case of partially satisfying sensitivity. Variables to be optimized were derived from the ELISA theory[60] and encompassed the quantity of the specific antibody and of the competitor. Usually, the antibody/competitor concentrations are defined upon maximizing their binding in the absence of the analyte. However, better performance in competitive ELISA have been achieved by optimizing simultaneously the competition ability along with the binding capability [61]. Similarly, we decided to investigate the variables both in the absence ("negative" sample) and in the presence of a certain amount of the analyte ("positive" sample), along the sequence of DoE. The 4S decision making process was based on the color intensity of the test line, which were defined as "intense", "faint" and "not visible". We included arbitrary thresholds (intense corresponds to signals ≥ 80 a.u., not visible to signals <15 a.u. in our measurement system, while signals comprised between 16 and 79 were classified as faint). Faint signals were considered as *false positive*, in case of "truly negative" sample, while they were assigned as *false negative* when they occurred with "truly positive" samples. On the other hand, intense test lines indicated a *true negative* in the case of a "truly negative" sample, while *not visible* test lines were considered *true positive* in the case of a "truly positive" sample. The co-presence of *true positives* and *true negatives* will be considered a satisfactory result in the 4S and will lead to a Stop, or to a Sharpen, of the process. In the absence of such conditions, the variables must be explored into another neighborhood of variables (Shift).

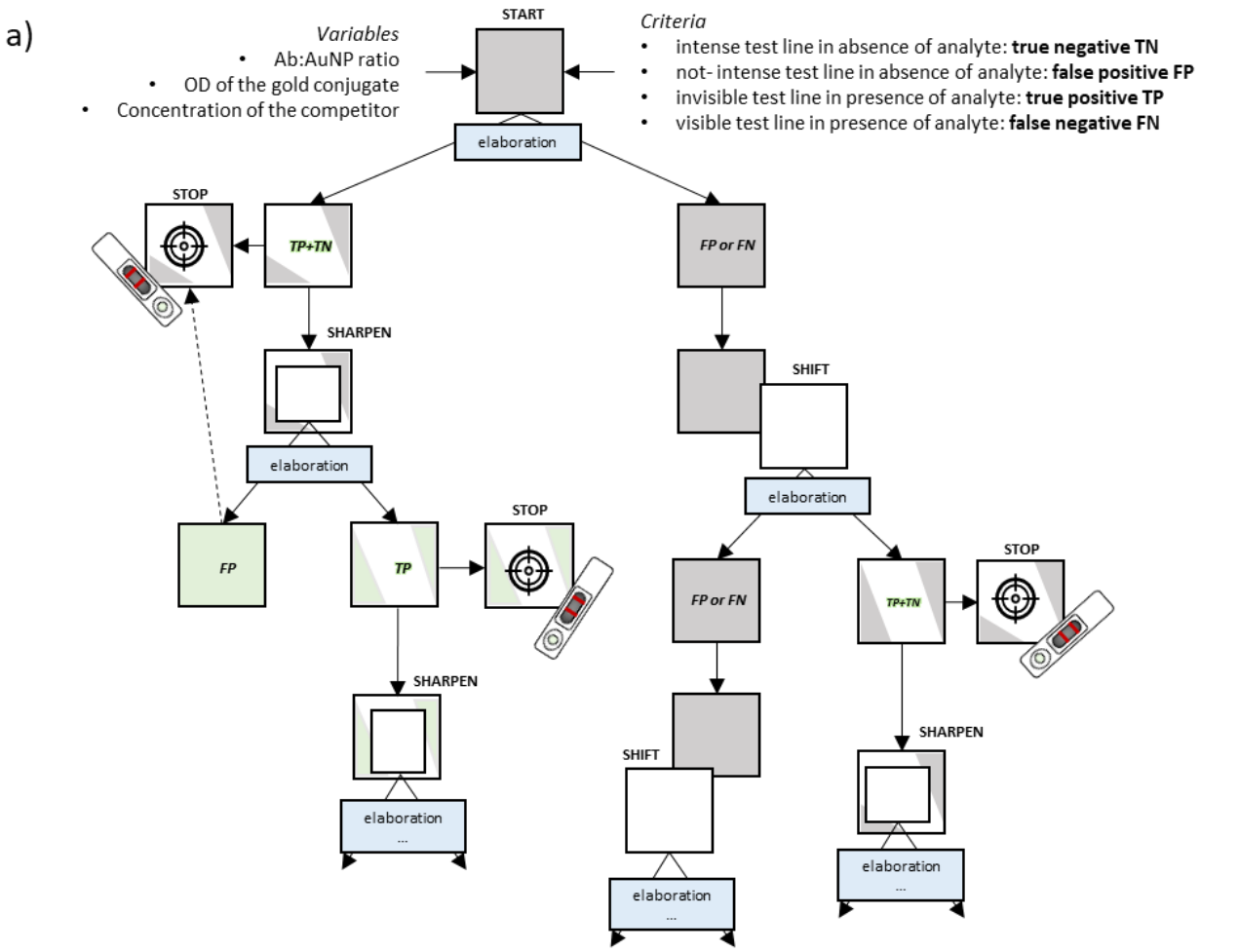

Figure 2: (a) Scheme of the '4S' strategy proposed in this work to optimize competitive LFIA and reach the highest analytical sensitivity through sequential DoEs. Once defined the target sensitivity level, a DoE is designed (START) and levels are investigated by analyzing a negative sample (no analyte) and a positive sample (containing the analyte at the target sensitivity). Results elaboration may include a TP+TN area (both the NEG and POS samples give back the expected results), in which variables combinations provide the desired LFIA performance (STOP). Eventually, a second DoE is designed and proven by using a lower concentration of the analyte (SHARPEN) to further improve the sensitivity (or enable lower reagents consumption). If unsatisfactory results are obtained by exploring the space in the DoEs, as no TP+TN areas are evidenced, the trends of the contour plot is used to identify a new variables space to be explored (SHIFT), and the process is iteratively repeated until reaching the goal. (b) Images of LFIA devices for the four results occurring at the test line: no analyte and signal ≥ 80 a.u (TN); no analyte, but signal < 80 a.u. (FP); analyte above the cut-off level and signal ≥ 15 a.u (FN), analyte above the cut-off level and signal < 15 a.u. (TP).

To illustrate the 4S approach and to verify the potential benefits for the development of truly sensitive visual competitive LFIAs, we applied it to redevelop a LFIA for the detection of cortisol in human saliva[62]. The original device included cortisol-BSA as the competitor (spotted to form the analyte-responsive sensitive line, test line), and a labelled anti-cortisol monoclonal antibody (linked to gold nanoparticles Ab_AuNP) as the label (**Figure 1c**). As previously reported, the LFIA was able to discriminate levels of cortisol above and below 4 ng/ml in human saliva. Nevertheless, the visual readout was based on comparing the intensity of the color at the test and the control lines (a second reactive line, incorporated into LFIA for assessing the functioning of the device) rather than on the disappearance of the test line. Although interesting, these performance were insufficient to meet requirements for diagnosing some specific pathological conditions and, above all, for applying the device to the ascertainment of stress in humans and animals, which require ultrahigh sensitive detection of salivary cortisol [63,64]. As an example, the diagnosis of the Cushing syndrome requires the measurement of night salivary cortisol, which cut-offs vary between 1.2 and 5.5 ng/mL [64–69]. Stress-related increase of cortisol have been reported in the range 2.0-10 ng/mL for humans, and variable levels are found in animals, from 0.6 at rest to 1.5ng/mL post training for horses[70], ranging 3.5-25 ng/ml for macaques depending on the stress condition[71]. The lowest concentration of cortisol detected in cattle saliva varied from 1.4 ng/ml [72] to 0.024 ng/ml[73].

In contrast to the use of different labels and detection techniques to improve the LFIA technique, at the expense of affordability, user-friendliness, deliverability, and/or by using equipment-dependent approaches, this strategy should allow to improve the sensitivity by disclosing the maximal potential of the employed immunoreagents and labels. Then, the aim of the work was to improve the performance of the device for the detection of cortisol and, at the same time, to establish a viable route for achieving high sensitivity by competitive LFIA, while maintaining unaltered the numerous advantages and the perfect adherence to the ASSURED criteria of visual devices. The use of the design of experiments in the optimization of an LFIA device represents an absolute novelty in the field of immunoassays. Moreover, its combination with the elaboration of a potentially universal decision strategy based on thresholds that can be easily adapted according to the required application makes this work a potential game changer for competitive immunoassay developers.

Experimental Section

Execution of the LFIA and acquisition of the analytical response

LFIA devices were fabricated as previously reported[53–55], with minor modifications detailed in the ESI.

For the development and optimization of the LFIA, standard solutions of cortisol diluted in the running buffer were used. Running buffer formulation was phosphate buffer 20 mM pH 7.4 supplemented by 1% w/v BSA

and 0.1% v/v Tween20. The assay execution consisted in the addition of 80µL of standard solution to the sample well and the evaluation of the results after 15 minutes of capillary flow (room temperature). The color intensity of the test lines was visually inspected and digitally acquired by means of a scanner (OpticSlim 550scanner, Plustek Technology GmbH, Norderstedt, Germany). The area including the colored lines was elaborated by means of QuantiScan 3.0 software (Biosoft, Cambridge, UK) and the area of the peak at the test and control lines was used as the "color intensity" expressed in arbitrary units.

Design of experiments for the optimization of the LFIA

Variables explored simultaneously investigated in the DoE were: the amount of the anti-cortisol antibody adsorbed onto AuNP (Ab), the amount of the conjugate included in the assay (measured as the optical density of the Ab-AuNP solution, OD) and the concentration of the cortisol-BSA spotted to form the test line (T). The number of experiments was defined by using the D-optimal algorithm similarly as previously described. [53] The first design (DoE I) included four levels of the Ab (4.0-2.0-1.0-0.5µg), three levels of OD (4-2-1), and 3 levels of T (1.0-0.5-0.2mg/mL), with a full-factorial number of 36 experiments, reduced at 13 experiments by D-optimal. The second design (DoE II) included three levels of Ab (1.0-0.5-0.25µg), three levels of OD (8-4-1), and 2 levels of T (0.1-0.05mg/mL), with a full-factorial 18 experiments, reduced at 13 experiments by D-optimal. The DoE III included two levels of Ab (0.25-0.10µg), two levels of OD (2-1), and 2 levels of T (0.05-0.025mg/mL), with a full-factorial 8 experiments, which was not reduced. In the different DoE, the levels were centered on the median value and coded considering simple function (linear, exp) connecting codes and values of the variables.

All the conditions were triple assessed in the presence of a defined concentration of cortisol (POS) and in the absence of analyte (NEG). The concentration of cortisol in the POS experiments was 1.0 ng/mL. The level of cortisol for the POS sample was reduced to 0.1 ng/mL (0.3 nM) in the DoE III. All experiments were done in duplicate and the mean intensity of the color at the test line was considered.

Chemometric Agile Tool software, developed by the Italian Group of Chemometrics (by Prof. Riccardo Leardi et al.) of the Italian Society of Chemistry (SCI), freely available on internet, within the R version 3.1.2 version, was employed to for multiple regression analysis (MLR) model computation and visualization (coefficient plots and response surfaces). The regression coefficients of the model that describes the effect of the variables (Ab, OD, T) on the response (R, the color intensity of test lines) was computed considered, other than the constant term (a_0), the linear effect of the three variables (a_1 to a_3), their pair combinations (a_3 to a_6), and the quadratic terms of the variables (a_7 to a_9):

$$R=a_0 + a_1\,Ab + a_2\,OD + a_3\,T + a_4\,Ab*OD + a_5\,Ab*T + a_6\,OD*T + a_7\,Ab^2 + a_8\,OD^2 + a_9\,T^2$$

For the DoE III, in which two levels for each variable have been considered, only the linear terms have been calculated.

The p-values of the regression coefficients were evaluated to identify the statistically significant parameters and to visualize the nature of the relationships of the parameters involved in the DoE. The significance of the variables within each DoE was visualized, with the convention of low * = p-value < 0.05, moderate ** = p-value < 0.01 and high significance *** = p-value < 0.005.

The experiments at the different experimental conditions were performed randomly to reduce the impact of potential systematic error on the calculated model.

LFIA for cortisol detection

Calibration curves were conducted by analyzing standard solutions of cortisol, in the range 0-10000 ng/mL for the unoptimized LFIA (LFIA 0), and 0-250 ng/mL for the optimized ones. The LFIA 0 condition represents a starting point for the development of the device were the immunoreagents are screened for their suitability into the expected format and main parameters are not optimized. The minimum stabilizing amount of antibody adsorbed onto AuNPs was used (4µg/OD), and standard concentration of probe (OD1) and competitor (1mg/mL) were used. It was used also to understand the optimization efficiency of the different depths of the employed 4S approaches.

Each calibrator was measured in three replicates. Calibration curves were fitted by means of four-parameters logistic curves using SigmaPlot 14.0 (Systat, Palo Alto, CA) software and the following parameters were calculated: color intensity in absence of cortisol (A_{max}), the half-maximal inhibition capacity (IC_{50}), dynamic range (IC_{20}-IC_{80}), and the visual limit of detection (vLOD). The vLOD was calculated by substituting the 15 a.u. in the 4PL model.

Reproducibility and stability of the LFIA 2.1

The between-batch variability of the LFIA 2.2 production was investigated by preparing three batches of LFIA device and measuring: λ_{max}, OD, width of localized surface plasmon resonance (LSPR) band of the Ab_AuNPs preparation and was expressed as the CV% (coefficient of variation). In addition, calibration curves were obtained from each batch and the CV% of the parameters (Amax, IC_{50}, Hill's slope), together with the CV% of the vLOD were calculated.

The stability of the LFIA was evaluated after 1-2-4-7 days of accelerated aging in dark bag storage at 37°C mimicking one year of room temperature aging. At each time point, the standard curves were assessed and the t_x/t_0 % were calculated for A_{max} and the vLOD.

Testing human saliva samples with the LFIA 2.1

The LFIA 2.1 device was used to analyze 9 human saliva samples. The sample collection was approved by the ethical committee (Prot. n. 0452970 del 28/07/2023). Participants in the study were kindly invited not to eat, smoke and drink in 30 minutes and not to do strong exercise in the 2 hours that preceded the saliva collection.

They were also asked to communicate the use of therapeutic drugs, especially in the case of hormonal drugs, such as contraceptives, corticosteroids and anabolic steroid drugs. Saliva samples were collected by using the SalivaBio Oral Swab from Salimetrics (Salimetric LLC, CA, USA) and following supplier's instructions. Collected samples were immediately refrigerated at 4°C and transported to the laboratory where they were stored at -20°C. For the analysis, samples were thawed at room temperature, centrifuged for 15 minutes at 2000 x g the resulting saliva extract was subjected to ELISA determination without any further treatments. The cortisol concentration in these samples was measured by means of a commercial ELISA kit [https://www.ibl-international.com/en/cortisol-saliva-elisa]. According to manufacturer, the limit of detection, the range of linearity, and the mean precision of the ELISA kit were 0.3 ng/mL, 0.5 - 30 ng/mL, and 13.2 %, respectively. For the LFIA testing of human saliva, samples were diluted 1:10 with the running buffer and applied to the device. Samples were analyzed in three replicates to examine the precision of the data. The recovery (R%) was calculated as

the ratio between the cortisol concentration obtained from the LFIA 2.1 and the one measured by the ELISA:

$$R\% = {[Cortisol\ (LFIA)]}\Big/{[Cortisol\ (ELISA)]} \times 100$$

Results and Discussion

The '4S' sequential optimization of the LFIA

A novel strategy denoted '4S' was proposed herewith aimed at allowing for rapidly (and cost-effectively) reaching the highest sensitivity achievable with a defined set of immunoreagents and materials (**Figure 2a**). Concerning the variables to be investigated, we took inspiration from the ELISA theory[60] and identified the following relevant factors affecting the sensitivity of competitive LFIA: (i) the concentration of the competitor (the antigen anchored onto the membrane to form the Test line), (ii) the concentration of the labelled bioligand (the specific antibody linked to AuNPs), and (iii) the modification index of the detector, which is the ratio between the antibody and the colorimetric label (AuNP). All these variables needed to be modulated to favor the competition, which implies maintaining a visible signal in the absence of the analyte (**"negative" sample**, NEG**)**, while no perceivable color at the test line was required to identify "positive" samples (POS), containing cortisol above a defined level). To convert these qualitative criteria into measurable signals, we decided two cut-off values according to the visual inspection of results. We arbitrary set 80 arbitrary units (a.u.) as the signal threshold corresponding to unequivocally colored lines, while signals below 15 a.u. were considered as undetectable as they were not visible by the unaided eye (**Figure 2b**). The cortisol cut-off value (1 ng/ml) was selected for the general purpose of developing a sensitive LFIA (the ng/mL is generally assumed as far beyond the sensitivity of the technique when small molecules are analyzed[13,14]) and for the particular application of detecting salivary cortisol at clinically relevant concentrations[68]. Responses were

classified as true negative (TN) if the NEG sample provided a colored line with intensity above 80 a.u., while conditions in which the NEG sample gave lower signals (< 80 a.u.) were classified as false positive (FP). In analogy, responses were classified as true positive (TP) if the POS sample provided an undetectable signal (< 15 a.u) and false negative (FN) in case of appreciable coloring of the test line (≥ 15 a.u). The existence of at least one combination of parameters that simultaneously fulfilled both criteria (TP+TN zones) was used as the indicator of achieved/not achieved goal, and guided decisions on following with additional DoE or not.

In the first DoE (DoE I), we explored four levels of Ab, and three levels of OD and T (**Table S2**). From a full factorial design including 36 experiments, 13 were selected by the D-optimal algorithm (**Figure S3**)**.** Among the NEG results, 100% were classified as TN, while the POS were 100% FN **(Table S3)**.

The computation, performed by means of CAT, of the models describing the test line color intensity for NEG and POS experiments showed explained variances of 91.4% and 92.7%, respectively, meaning a good fitting of the experimental dataset. The Ab and OD variables resulted in low and moderate positive correlation, respectively, while T was lowly (p-value > 0.05) and negatively correlated **(Figure S4).** The coefficient plot was similar in POS and NEG experiments, which means that, in the considered intervals, variables were not useful to increase the sensitivity. By observing the response surfaces **(Figure S5)**, a small sector among the predicted combinations could be individuated that fulfilled the criteria of TP+TN. The central condition of this area was decodified as Ab=-1 (0.5 μg); OD=-0.5 (1.375); T=-1 (0.25mg/mL) and will be hereafter referred to as LFIA 1.

According to the 4S strategy, a second DoE (DoE II) was designed to explore a different combination of variables (SHIFT), which included three lower Ab levels (0.25-1.0μg), a wider OD range (1-8), and lower T levels (0.05-0.1mg/mL) **(Table S4).** From the full factorial design including 18 experiments, 13 were selected by the D-optimal algorithm **(Figure S6).** From this set of experiments, most results (11 out of 13) were classified as TN and FN, while 2 were characterized by a TP and FP response **(Table S5).**

The computation of the models describing the NEG and POS experiments showed, again, good fitting (99.56% and 94.43%, respectively). The coefficient plot considered Ab and OD levels as highly significant (*** = p-value < 0.005) in NEG experiments, whereas the significance decreased in POS experiments (** = p-value < 0.01) **(Figure S7).** By mapping the response surfaces, despite the absence of TP+TN combinations among the experiments, wider areas were found predicting TP+TN, compared with DoE I (**Figure S8**), especially for low T and moderate Ab and OD (**Figure 3**).

We, then, decided to zoom in the variables inside the TN+TP region individuated by the DoE II, exploring lower levels of T. Thus, a third experimental set, DoE III, was performed without cutting algorithm. Moreover, the POS criterium was made more stringent (0.1 ng/mL of cortisol), with the aim of pursuing higher sensitivity (SHARPEN)**.** The eight experiments were the combinations of two levels of each variable **(Table S6)**. The experimental results classified 4 combinations as TN and 4 as FP among the NEG, while none of the experiments gave signals < 15 a.u. in the presence of 0.1 ng/mL of cortisol (100% FN) (**Table S7**). We concluded that we had reached the limit of sensitivity compatible with the bioreagents and materials we had

(STOP). The inhibition of the test line color in the presence of 0.1 ng/mL of cortisol compared to the NEG sample ranged between 15 % and 44 %. The model computation was, once more, characterized by good fitting (97.1% and 97.2% for NEG and POS, respectively), but the coefficient plot evidenced that no variables was significant in the description of the variation of the color intensity of test line (**Figure S9**). That is, the computed model was not statistically reliable to describe the system. The response surface mapping showed no TN+TP (**Figure S10)**. Therefore, the best combination was individuated among the ones giving the lowest POS signal in TN areas (**Table S8**). Two conditions were found that provided the maximal signal inhibition and were indicated hereafter as LFIA 2.1 (Ab: 0.12 µg, OD: 1.0, T: 0.05 mg/mL) and LFIA 2.2 (Ab: 0.1 µg, OD: 1.25, T: 0.05 mg/mL).

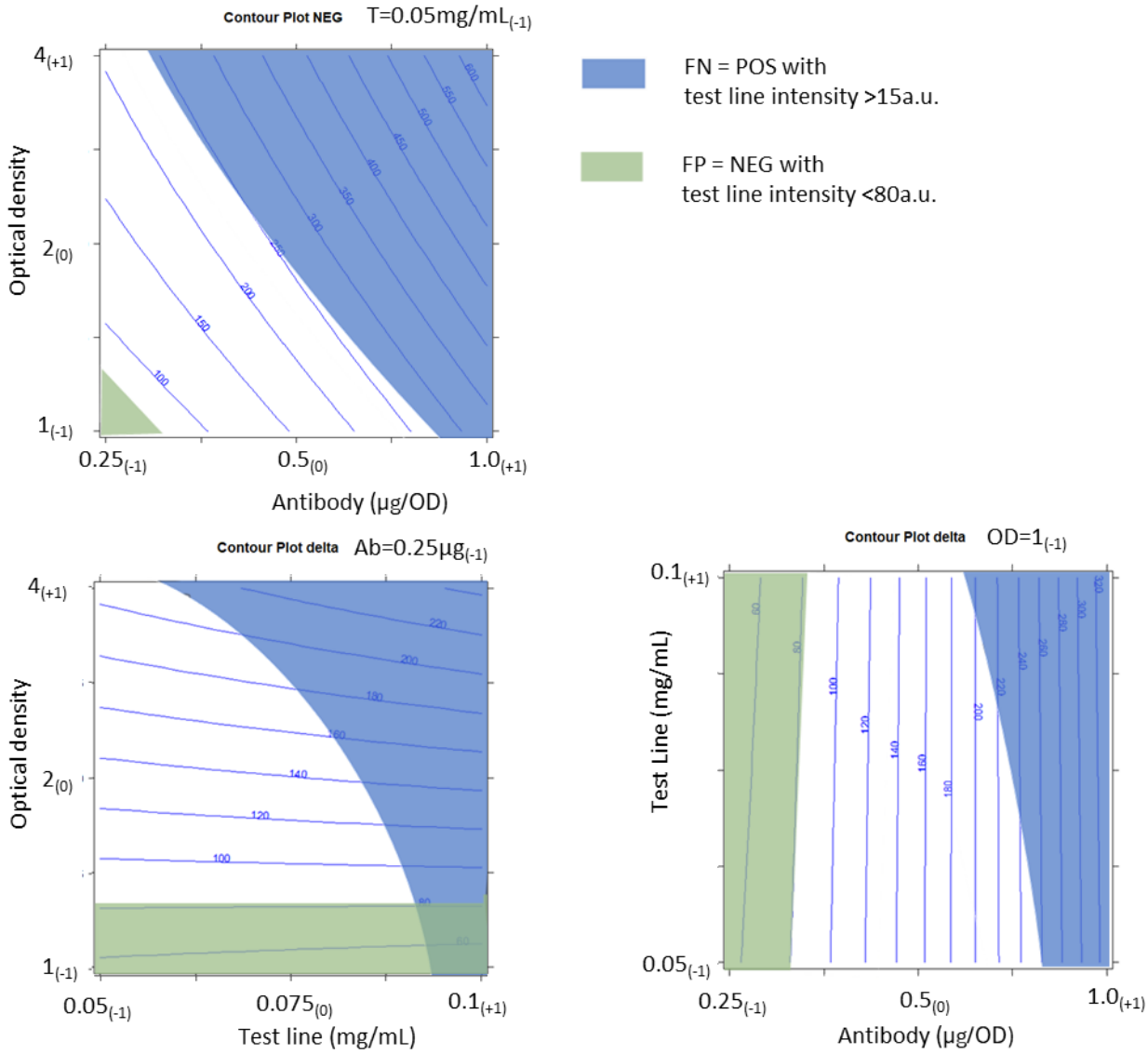

Figure 3: Detail of the TN+TP zones in the elaboration of the DoE II. Levels refers to the signal of the NEG, the blue space is the FN area, while the green space is the FP area. Countour plots are shown for a fixed level (-1) of one of the variables (corresponding to T=0,05 mg/mL; Ab=0,25 ug; OD=1).

Comparing the LFIA generations: the effect of the 4S process on the sensitivity

To check the effectiveness of the 4S strategy, we built four calibration curves for measuring cortisol by using three LFIA devices, based on differently optimized combinations of bioreagents: the starting LFIA 0 prepared by adsorbing the stabilizing amount of Ab (4 µg) to AuNPs, at the highest explored OD level (4), and the highest explored concentration of the competitor (1 mg/mL); the LFIA 1, which was the optimized device obtained after the first DoE elaboration; and two LFIA 2, obtained at the end of the 4S process. Combinations were compared in terms of their analytical performances and reagents consumption **(Table 1)**.

Table 1: Comparison of the characteristics and analytical performances of the calibration curves prepared for the different LFIA generations.

		LFIA 0	LFIA 1	LFIA 2.1	LFIA 2.2
variables	Ab (µg/OD)	4.0	0.5	0.12	0.1
	Optical density (a.u.)	4.0	1.4	1.0	1.3
	Test line concentration (mg/mL)	1.0	0.2	0.05	0.05
figures-of-merit	Visual limit of detection, vLOD[1] (ng/mL)	>10000	20.5 ± 1.0	2.2 ± 0.1	2.0 ± 0.1
	A_{max} [2] (a.u.)	560 ± 28	217 ± 9	83 ± 6	85 ± 3
	Hill's slope	n.d.[3]	-1.13 ± 0.25	-1.05 ± 0.23	-1.10 ± 0.22
	Half-max. inhibition concentration, IC_{50} (ng/mL)	n.d.	1.9 ± 0.4	0.5 ± 0.1	0.5 ± 0.1
	Dynamic range, IC_{20}-IC_{80} (ng/mL)	n.d.	6.6 – 0.6	1.9 – 0.1	1.7 – 0.1
	Limit of detection, LOD[4] (ng/mL)	n.d.	0.28	0.06	0.07
	Antibody consumption (ng/test)	480.0	20.6	3.6	3.8
	Competitor consumption (ng/test)	400.0	80.0	20.0	20.0

[1]Calculated as the concentration of cortisol providing a Test line signal = 15 a.u.
[2]Signal of the blank (no cortisol)
[3]n.d.: not determinable
[4]Calculated as the concentration providing a 10% inhibition of the signal (IC_{90})

The LFIA 0 showed negligible inhibition (28.6%) even at an extremely high concentration of cortisol (10000 ng/mL) (**Figure 4a**) and parameters of the logistic equation and the vLOD could not be estimated. On the contrary, the LFIA 1 showed adequate analytical performances **(Figure 4b)**. In fact, a very intense signal was observed in the absence of analyte (217 ± 28 a.u.) and the IC_{50} (1.9 ± 0.4 ng/mL) fitted with clinically relevant concentrations of cortisol [64,66–68,70,71,74–81]. The device enabled cortisol detection with a dynamic range between 0.6 ng/mL and 6.6 ng/mL. Most importantly for the application of the LFIA as a qualitative assay with visual inspection of results, the vLOD was calculated as 20.5 ± 1.0 ng/mL.

The reagent consumption was 20.6 ng/test of antibody and 80 ng/test of competitor (antigen), which were 23.3-fold and 5-fold lower, respectively, compared to the ones used in the LFIA 0.

The LFIA 2.1 represented a significant further improvement over the LFIA 1 **(Figure 4c)**. In the absence of analyte, a clearly visible colored line could still be appreciated (83 ± 6 a.u.) and the IC_{50} improved (0.5 ± 0.1 ng/mL). The dynamic interval ranged between 0.1 ng/mL and 1.9 ng/mL. The vLOD also improved by an order of magnitude and was estimated down to 2.2 ± 0.1 ng/mL. The limit of detection (LOD) of the LFIAs improved from the LFIA 0 (not computable), to the LFIA 1 (0.28ng/mL) up to the LFIA 2.1 and LFIA 2.3 that showed similar values and a significant improvement (0.06 and 0.07 ng/mL, respectively). The reagent consumption was 3.6 ng/test of antibody and 20 ng/test of competitor, which were 5.7-fold and 4-fold lower, respectively, compared with the ones employed in the LFIA 1 and more than 130-folds and 20-folds lower, respectively, than those used to produce the LFIA 0. The LFIA 2.2 showed results comparable to the ones obtained with the LFIA 2.1 **(Figure 4d).**

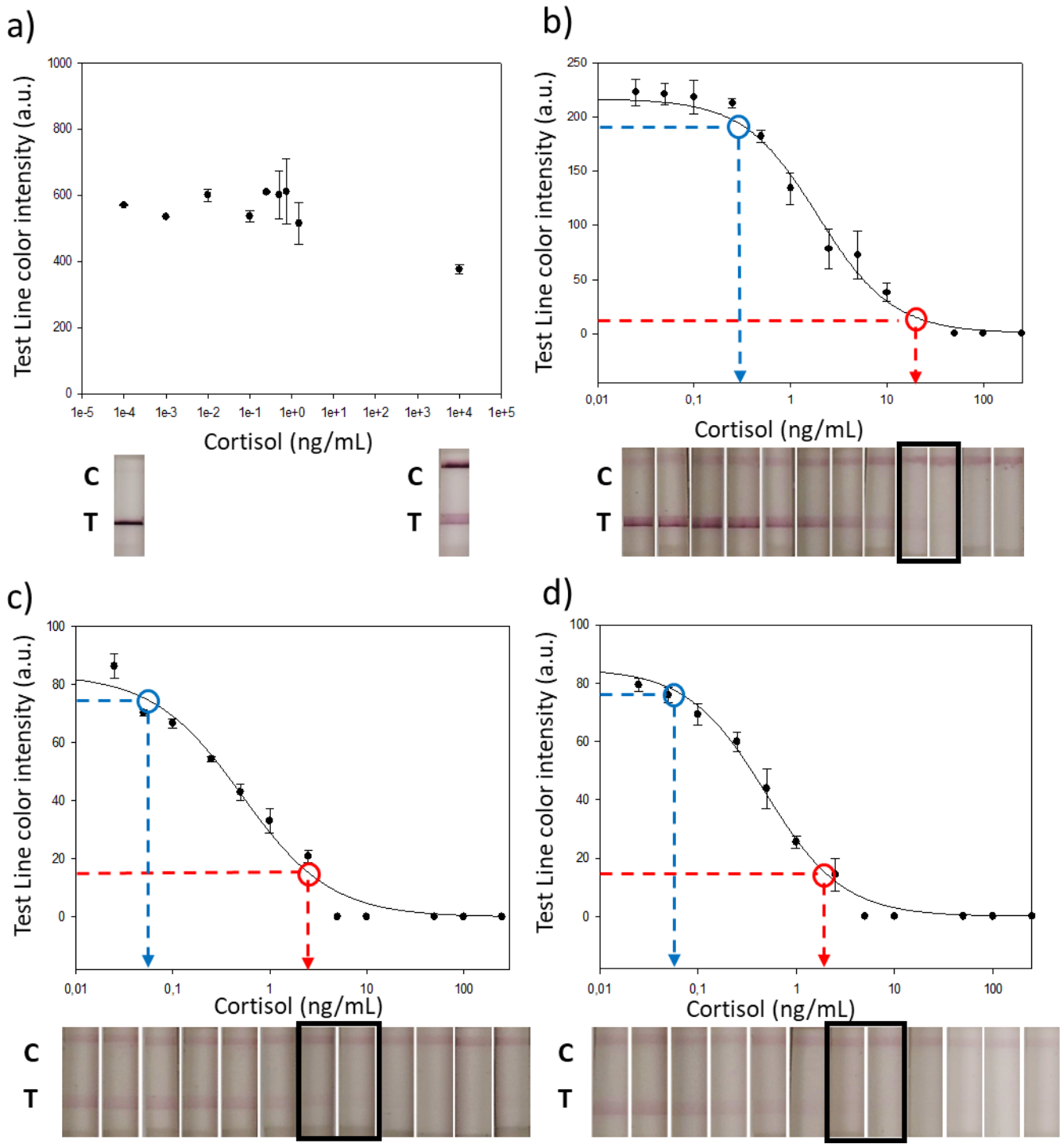

Figure 4: Calibration curves prepared by using unoptimized conditions (LFIA 0, a), and conditions obtained trough the application of the 4S strategy: LFIA 1 (b), LFIA 2.1 (c), and LFIA 2.2 (d). All the standard solution were triple tested and the error bars represent the standard deviation. Blue dashed lines and circles indicates the LOD (IC_{90}), red dashed lines and circles indicates the visual LOD (test line intensity = 15 a.u.)

Summarizing, the 4S strategy, which, in this case, included 3 sequential experimental designs (**Figure 5**), allowed us to achieve a sensitivity improvement by a factor >5000 compared to the unoptimized condition, with an about 40-fold lower overall bioreagents consumption, while using the same materials and immunoreagents.

The overall number of experiments carried out was 34, which could be an acceptable effort given the dramatic sensitivity improvement achieved through them and demonstrates the power of a systematic unbiased approach. It is worthwhile noticing that limiting to the application of one round of DoE implied surrendering one order of magnitude in terms of vLOD to save 21 experiments.

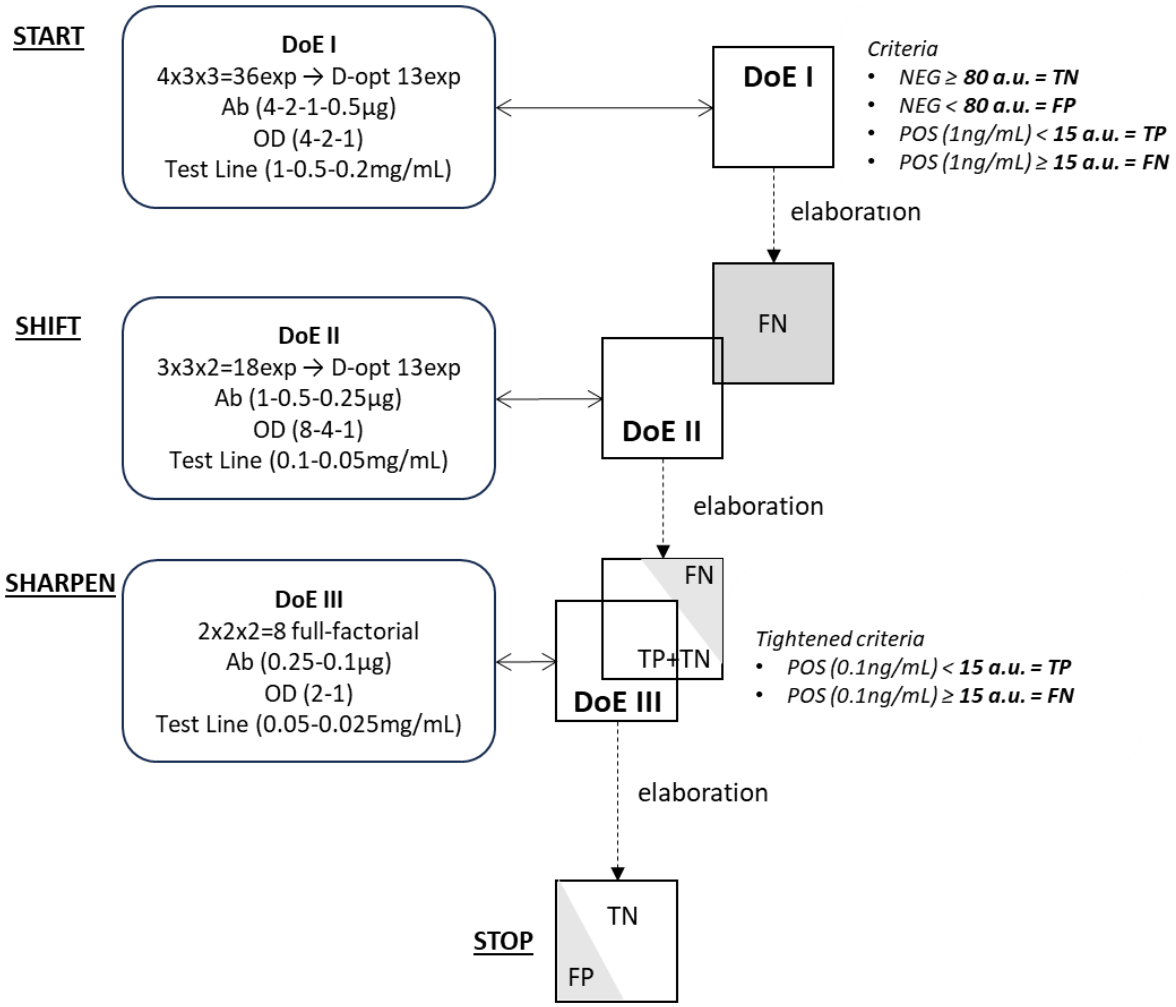

Figure 5: The 4S strategy followed in this work. From DoE I (START), we shifted towards DoE II. The DoE III was a SHARPEN of DoE II and enabled reaching the satisfying sensitivity (STOP).

Reproducibility and stability of the LFIA 2.1

As the quantity of the antibody adsorbed onto the AuNP to produce optimized LFIA was far lower than the stabilizing amount, the robustness of the probe and the reproducibility of the results was questioned. Therefore, the conjugation of the Ab and AuNP was repeated trice, and the conjugates were characterized by Vis spectroscopy. The shape and maximum of the LSPR bands were consistent among preparations (CV% of the λ_{max} of 0.03%).

At the same time, the reproducibility of the LFIA 2.1 was evaluated by preparing three batches of the device and obtaining a calibration curve for each batch. The 4PL parameters for the three curves were compared

and showed very consistent results (**Table S9)** with CV% below 10% for all considered parameters. A slightly lower reproducibility resulted in the vLOD (CV% = 12.6 %).

Finally, the stability overtime was verified for the LFIA 2.1 device after 1-2-4-7 days of accelerated aging at 37°C (**Figure S11).**

Results from testing human saliva samples with the LFIA 2.1

To assess the practical application of the optimized LFIA, it was applied to measure cortisol in human saliva, which is a representative complex biological fluid in which, furthermore, high sensitivity is required because cortisol is found in low concentrations [64–67]. A total of 9 human saliva samples were analyzed for their cortisol concentration by means of a commercial ELISA kit. The concentration of 8 out of the 9 human samples (s1-8) ranged between 2.1 ng/mL and 6.6 ng/mL, while 1 sample was below the limit of detection (s0). Samples were also analyzed by the optimized LFIA (LFIA 2.1) after 1:10 dilution in the running buffer. The quantification of the cortisol concentration was made by interpolating test line intensity values into the 4-PL calibration curve, and the agreement of results with the reference values was expressed as recovery (%). The recovery ranged between 70-109% (**Table S10**) and the s0 was below the LOD of the LFIA 2.1 consistently with ELISA result. Also considering the average precision of the reference ELISA kit (13.2%), results obtained by the LFIA 2.1 were adequate. It should be remarked also that we did not study the matrix effect of human saliva on the LFIA 2.1 and simply applied a 1:10 dilution to limit possible interference. Notwithstanding, the results provided by the optimized and highly sensitive LFIA 2.1 were consistent with the ELISA quantification so proving its feasibility for real world applications.

Conclusions

We proposed a general route to develop and optimize competitive visual LFIA based on the use of DoE combined in the "4S" approach. In the presented case of study, the application of the 4S strategy allowed us to achieve remarkably improved analytical performances with a limited number of experiments. Starting with a not optimized condition (LFIA 0) they would have been considered underperforming. In fact, using the minimum stabilizing amount of antibody adsorbed onto AuNPs, and standard concentration of probe and competitor the inhibition 4PL curve is not appreciable into clinically relevant concentration of cortisol. The suitable sensitivity was reached by a factor of >500 after only 13 experiments, and then improved up to >5000 after 34 experiments. The unparallelled visual LFIA performance reached through this approach are comparable to those obtained by using instrumental processing of images and/or complicated assay protocols (**Table S11**). Moreover, the reagents consumption for each test was reduced by a factor of ca. 40. The strategy included the definition of two levels of the analyte concentration to be used in the evaluation of DoE results, and a flowchart and rules to guide the optimization process.

The variables that mostly affected the LFIA sensitivity were the concentration of the competitor forming the test line and the amount of the antibody adsorbed per unit of gold nanoparticles, whereas the quantity of the labelled antibody was shown to impact in a lesser extent on the assay sensitivity.

Interestingly, comparing competitive ELISA and LFIA techniques, parameters affected differently the sensitivity of the assays **(Table 2)**. In fact, the optimization of competitive ELISAs usually involves the optimization of the amount of the antibody and the competitor, and the decrease of one or both reagents is considered as the straightforward strategy to improve the sensitivity[82]. In the LFIA technique, lowering the absolute amount of the labelled antibodies seemed less effective, except in cases where the decrease was obtained by adsorbing less antibody per AuNP unit.

Table 2: Impact of variables on the sensitivity of the ELISA[82] and LFIA

Variable	Influence on sensitivity	
	ELISA	LFIA
Concentration of the labelled antibody	high	low
Antibody-to-label ratio	high	moderate
Concentration of the competitor	high	high

Other parameters have been reported to influence the performance of competitive LFIAs, such as nitrocellulose membrane porosity and capillary flow rate[42]. These factors have been thoroughly investigated and their effects are well established. Another important point to consider is the study of the matrix effect, which includes the nature of the biological sample being analyzed, its viscosity, the presence of interfering compounds, etc[10]. Although this work focused on the methodological approach to achieve high sensitivity, we have shown that the optimized LFIA 2.1 is suitable for the measurement of cortisol in the presence of a complex matrix such as human saliva. Although the experiments were performed on a limited number of samples, they confirmed that the optimized device retains its functionality in real-world applications, in addition to the advantages in terms of speeding up the optimization process and allowing low consumption of costly reagents.

The implications of this work are generalizable **to the field of competitive LFIA development. In fact, any measurable signal can replace the** color **intensity of the test line used here to illustrate the approach; it is sufficient to define a reasonable working range for the variables for the 4S process and thresholds for interpretation to allow devices to be** optimized **with few resources.** This approach applies to the development of any diagnostic device that provides results in terms of signal inhibition by competing reagents.

Declaration of competing interest

The authors declare that they have no known competing financial interests or personal relationships that could have appeared to influence the work reported in this paper.

Data availability statement

Data will be made available on request.

Author contribution statement

All the co-authors have contributed and approved this final version of the manuscript

Acknowledgements and fundings

- This research acknowledges support from Project CH4.0 under the MUR program “Dipartimenti di Eccellenza 2023-2027” (CUP:D13C22003520001)

References

[1] B. G. Andryukov, Six decades of lateral flow immunoassay: from determining metabolic markers to diagnosing COVID-19, AIMS Microbiol. 6 (2020) 280–304. https://doi.org/10.3934/microbiol.2020018.

[2] C.M. Plotz, J.M. Singer, The latex fixation test: II. Results in rheumatoid arthritis, Am. J. Med. 21 (1956) 893–896. https://doi.org/10.1016/0002-9343(56)90104-8.

[3] L. Khelifa, Y. Hu, N. Jiang, A.K. Yetisen, Lateral flow assays for hormone detection, Lab Chip. 22 (2022) 2451–2475. https://doi.org/10.1039/D1LC00960E.

[4] A. Mohammadinejad, S. Nooranian, R. Kazemi Oskuee, S. Mirzaei, G. Aleyaghoob, A. Zarrabi, E. Selda Gunduz, Y. Nuri Ertas, M.A. Sheikh Beig Goharrizi, Development of Lateral Flow Assays for Rapid Detection of Troponin I: A Review, Crit. Rev. Anal. Chem. (2022) 1–15. https://doi.org/10.1080/10408347.2022.2144995.

[5] B. Ince, M.K. Sezgintürk, Lateral flow assays for viruses diagnosis: Up-to-date technology and future prospects, TrAC Trends Anal. Chem. 157 (2022) 116725. https://doi.org/10.1016/j.trac.2022.116725.

[6] B. Bruijns, R. Tiggelaar, J. Knotter, A. van Dam, Use of Lateral Flow Assays in Forensics, Sensors. 23 (2023) 6201. https://doi.org/10.3390/s23136201.

[7] H. Boutal, C. Moguet, L. Pommiès, S. Simon, T. Naas, H. Volland, The Revolution of Lateral Flow Assay in the Field of AMR Detection, Diagnostics. 12 (2022) 1744. https://doi.org/10.3390/diagnostics12071744.

[8] G. Xing, X. Sun, N. Li, X. Li, T. Wu, F. Wang, New Advances in Lateral Flow Immunoassay (LFI) Technology for Food Safety Detection, Molecules. 27 (2022) 6596. https://doi.org/10.3390/molecules27196596.

[9] F. Di Nardo, M. Chiarello, S. Cavalera, C. Baggiani, L. Anfossi, Ten Years of Lateral Flow Immunoassay Technique Applications: Trends, Challenges and Future Perspectives, Sensors. 21 (2021) 5185. https://doi.org/10.3390/s21155185.

[10] M. Sajid, A.-N. Kawde, M. Daud, Designs, formats and applications of lateral flow assay: A literature review, J. Saudi Chem. Soc. 19 (2015) 689–705. https://doi.org/10.1016/j.jscs.2014.09.001.

[11] B. O'Farrell, Lateral Flow Immunoassay Systems: Evolution from the Current State of the Art to the Next Generation of Highly Sensitive, Quantitative Rapid Assays, Immunoass. Handb. Theory Appl. Ligand Bind. ELISA Relat. Tech. (2013) 89–107. https://doi.org/10.1016/B978-0-08-097037-0.00007-5.

[12] G. Wu, M.H. Zaman, G. Wu, M.H. Zaman, Low-cost tools for diagnosing and monitoring HIV infection in low-resource settings, Bull. World Health Organ. 90 (2012) 914–920. https://doi.org/10.2471/BLT.12.102780.

[13] X. Yin, S. Liu, D. Kukkar, J. Wang, D. Zhang, K.-H. Kim, Performance enhancement of the lateral flow immunoassay by use of composite nanoparticles as signal labels, TrAC Trends Anal. Chem. 170 (2024) 117441. https://doi.org/10.1016/J.TRAC.2023.117441.

[14] D. Lou, L. Fan, T. Jiang, Y. Zhang, Advances in nanoparticle-based lateral flow immunoassay for point-of-care testing, View. 3 (2022) 20200125. https://doi.org/10.1002/VIW.20200125.

[15] K.M. Mayer, J.H. Hafner, Localized surface plasmon resonance sensors, Chem. Rev. 111 (2011) 3828–3857. https://doi.org/10.1021/CR100313V.

[16] E.C. Dreaden, A.M. Alkilany, X. Huang, C.J. Murphy, M.A. El-Sayed, The golden age: gold nanoparticles for biomedicine, Chem. Soc. Rev. 41 (2012) 2740–2779. https://doi.org/10.1039/C1CS15237H.

[17] N. Sarfraz, I. Khan, Plasmonic Gold Nanoparticles (AuNPs): Properties, Synthesis and their Advanced Energy, Environmental and Biomedical Applications, Chem Asian J. 16 (2021) 720–742. https://doi.org/10.1002/asia.202001202.

[18] X. Chen, X. Miao, T. Ma, Y. Leng, L. Hao, H. Duan, J. Yuan, Y. Li, X. Huang, Y. Xiong, Gold nanobeads with enhanced absorbance for improved sensitivity in competitive lateral flow immunoassays, Foods. 10 (2021) 1488. https://doi.org/10.3390/FOODS10071488/S1.

[19] N. Yao, X. Li, Y. Tian, Z. Huang, Y. Duan, Core-shell Au@PdNPs based colorimetric enhanced lateral flow immunoassay for C-reactive protein detection, Sensors Actuators B Chem. 379 (2023) 133247. https://doi.org/10.1016/J.SNB.2022.133247.

[20] Q. Huang, L. Dang, Graphene-labeled synthetic antigen as a novel probe for enhancing sensitivity

546 and simplicity in lateral flow immunoassay, Anal. Methods. 14 (2022) 1155–1162.
547 https://doi.org/10.1039/D1AY02158C.
548 [21] Y. Zhong, Y. Chen, L. Yao, D. Zhao, L. Zheng, G. Liu, Y. Ye, W. Chen, Gold nanoparticles based lateral
549 flow immunoassay with largely amplified sensitivity for rapid melamine screening, Microchim. Acta.
550 183 (2016) 1989–1994. https://doi.org/10.1007/S00604-016-1812-9/FIGURES/3.
551 [22] S. Ruantip, U. Pimpitak, S. Rengpipat, E. Pasomsub, C. Seepiban, O. Gajanandana, P. Torvorapanit, N.
552 Hirankarn, P. Jaru-ampornpan, S. Siwamogsatham, P. Pongpaibool, S. Siwamogsatham, N.
553 Thongchul, S. Chaiyo, Self-enhancement lateral flow immunoassay for COVID-19 diagnosis, Sensors
554 Actuators B Chem. 389 (2023) 133898. https://doi.org/10.1016/J.SNB.2023.133898.
555 [23] N.A. Byzova, I. V. Safenkova, E.S. Slutskaya, A. V. Zherdev, B.B. Dzantiev, Less is More: A Comparison
556 of Antibody-Gold Nanoparticle Conjugates of Different Ratios, Bioconjug. Chem. 28 (2017) 2737–
557 2746. https://doi.org/10.1021/acs.bioconjchem.7b00489.
558 [24] A. Gumustas, M.G. Caglayan, M. Eryilmaz, Z. Suludere, E. Acar Soykut, B. Uslu, I.H. Boyaci, U. Tamer,
559 Paper based lateral flow immunoassay for the enumeration of Escherichia coli in urine, Anal.
560 Methods. 10 (2018) 1213–1218. https://doi.org/10.1039/C7AY02974H.
561 [25] E. Eltzov, R.S. Marks, Colorimetric stack pad immunoassay for bacterial identification, Biosens.
562 Bioelectron. 87 (2017) 572–578. https://doi.org/10.1016/j.bios.2016.08.044.
563 [26] R. Chen, H. Wang, C. Sun, Y. Zhao, Y. He, M.S. Nisar, W. Wei, H. Kang, X. Xie, C. Du, Q. Luo, L. Yang, X.
564 Tang, B. Xiong, Au@SiO2 SERS nanotags based lateral flow immunoassay for simultaneous detection
565 of aflatoxin B1 and ochratoxin A, Talanta. 258 (2023) 124401.
566 https://doi.org/10.1016/j.talanta.2023.124401.
567 [27] A. Raysyan, I.A. Galvidis, R.J. Schneider, S.A. Eremin, M.A. Burkin, Development of a latex particles-
568 based lateral flow immunoassay for group determination of macrolide antibiotics in breast milk, J.
569 Pharm. Biomed. Anal. 189 (2020) 113450. https://doi.org/10.1016/j.jpba.2020.113450.
570 [28] S.-A. Jin, Y. Heo, L.-K. Lin, A.J. Deering, G.T.-C. Chiu, J.P. Allebach, L.A. Stanciu, Gold decorated
571 polystyrene particles for lateral flow immunodetection of Escherichia coli O157:H7, Microchim. Acta.
572 184 (2017) 4879–4886. https://doi.org/10.1007/s00604-017-2524-5.
573 [29] O.D. Hendrickson, E.A. Zvereva, B.B. Dzantiev, A. V. Zherdev, Highly Sensitive
574 Immunochromatographic Detection of Porcine Myoglobin as Biomarker for Meat Authentication
575 Using Prussian Blue Nanozyme, Foods. 12 (2023) 4252. https://doi.org/10.3390/foods12234252.
576 [30] Q. Huang, L. Dang, Graphene-labeled synthetic antigen as a novel probe for enhancing sensitivity
577 and simplicity in lateral flow immunoassay, Anal. Methods. 14 (2022) 1155–1162.
578 https://doi.org/10.1039/D1AY02158C.
579 [31] V.S. Garcia, S.A. Guerrero, L.M. Gugliotta, V.D.G. Gonzalez, A lateral flow immunoassay based on
580 colored latex particles for detection of canine visceral leishmaniasis, Acta Trop. 212 (2020) 105643.

https://doi.org/10.1016/j.actatropica.2020.105643.
[32] C. Parolo, A. Sena-Torralba, J.F. Bergua, E. Calucho, C. Fuentes-Chust, L. Hu, L. Rivas, R. Álvarez-Diduk, E.P. Nguyen, S. Cinti, D. Quesada-González, A. Merkoçi, Tutorial: design and fabrication of nanoparticle-based lateral-flow immunoassays, Nat. Protoc. 15 (2020) 3788–3816. https://doi.org/10.1038/s41596-020-0357-x.
[33] T. Salminen, F. Mehdi, D. Rohila, M. Kumar, S.M. Talha, J.A.J. Prakash, N. Khanna, K. Pettersson, G. Batra, Ultrasensitive and Robust Point-of-Care Immunoassay for the Detection of Plasmodium falciparum Malaria, Anal. Chem. 92 (2020) 15766–15772. https://doi.org/10.1021/acs.analchem.0c02748.
[34] R. Chen, C. Ren, M. Liu, X. Ge, M. Qu, X. Zhou, M. Liang, Y. Liu, F. Li, Early Detection of SARS-CoV-2 Seroconversion in Humans with Aggregation-Induced Near-Infrared Emission Nanoparticle-Labeled Lateral Flow Immunoassay, ACS Nano. 15 (2021) 8996–9004. https://doi.org/10.1021/acsnano.1c01932.
[35] N. Cheng, Y. Song, M.M.A. Zeinhom, Y.-C. Chang, L. Sheng, H. Li, D. Du, L. Li, M.-J. Zhu, Y. Luo, W. Xu, Y. Lin, Nanozyme-Mediated Dual Immunoassay Integrated with Smartphone for Use in Simultaneous Detection of Pathogens, ACS Appl. Mater. Interfaces. 9 (2017) 40671–40680. https://doi.org/10.1021/acsami.7b12734.
[36] H. Ilhan, B. Guven, U. Dogan, H. Torul, S. Evran, D. Çetin, Z. Suludere, N. Saglam, İ.H. Boyaci, U. Tamer, The coupling of immunomagnetic enrichment of bacteria with paper-based platform, Talanta. 201 (2019) 245–252. https://doi.org/10.1016/j.talanta.2019.04.017.
[37] T. Axelrod, E. Eltzov, R.S. Marks, Capture-Layer Lateral Flow Immunoassay: A New Platform Validated in the Detection and Quantification of Dengue NS1, ACS Omega. 5 (2020) 10433–10440. https://doi.org/10.1021/acsomega.0c00367.
[38] H.J. Goux, B. V. Vu, K. Wasden, K. Alpadi, A. Kumar, B. Kalra, G. Savjani, K. Brosamer, K. Kourentzi, R.C. Willson, Development of a quantitative fluorescence lateral flow immunoassay (LFIA) prototype for point-of-need detection of anti-Müllerian hormone, Pract. Lab. Med. 35 (2023) e00314. https://doi.org/10.1016/j.plabm.2023.e00314.
[39] C. Chen, J. Wu, A Fast and Sensitive Quantitative Lateral Flow Immunoassay for Cry1Ab Based on a Novel Signal Amplification Conjugate, Sensors. 12 (2012) 11684–11696. https://doi.org/10.3390/s120911684.
[40] L. Wu, J. Liang, P. Teng, Y. Du, Y. He, S. Liao, J. Wang, X. Zhang, Z. Wang, T. Zeng, Y. Wang, S. Zou, C. Lu, A. Jia, Q. Song, B. Huang, L. Fang, W. Cheng, Y. Tang, A filter pad design-based multiplexed lateral flow immunoassay for rapid simultaneous detection of PDCoV, TGEV, and PEDV in swine feces, Talanta. 280 (2024) 126712. https://doi.org/10.1016/j.talanta.2024.126712.
[41] X. Cai, Y. Luo, C. Zhu, D. Huang, Y. Song, Rhodium nanocatalyst-based lateral flow immunoassay for

616 sensitive detection of staphylococcal enterotoxin B, Sensors Actuators B Chem. 367 (2022) 132066.
617 https://doi.org/10.1016/j.snb.2022.132066.
618 [42] N.-D. Duong, K.-H. Nguyen-Phuoc, K.-Y.T. Do, T.-D. Mai-Hoang, N.-T.T. Nguyen, T.L. Tran, H. Tran-
619 Van, A Protocol for the Optimization of Lateral Flow Immunoassay Strip Development, Biomed. Res.
620 Ther. 10 (2023) 5500–5508. https://doi.org/10.15419/bmrat.v10i1.788.
621 [43] H. Xu, L. Zheng, Y. Xie, H. Zeng, Q. Fan, B. Zheng, Y. Zhang, Identification and determination of
622 glycoprotein of edible brid's nest by nanocomposites based lateral flow immunoassay, Food Control.
623 102 (2019) 214–220. https://doi.org/10.1016/j.foodcont.2019.03.018.
624 [44] W. Li, Z. Wang, X. Wang, L. Cui, W. Huang, Z. Zhu, Z. Liu, Highly efficient detection of deoxynivalenol
625 and zearalenone in the aqueous environment based on nanoenzyme-mediated lateral flow
626 immunoassay combined with smartphone, J. Environ. Chem. Eng. 11 (2023) 110494.
627 https://doi.org/10.1016/j.jece.2023.110494.
628 [45] L. Anfossi, C. Baggiani, C. Giovannoli, F. Biagioli, G. D'Arco, G. Giraudi, Optimization of a lateral flow
629 immunoassay for the ultrasensitive detection of aflatoxin M1 in milk, Anal. Chim. Acta. 772 (2013)
630 75–80. https://doi.org/10.1016/j.aca.2013.02.020.
631 [46] B. Ngom, Y. Guo, X. Jin, D. Shi, Y. Zeng, T. Le, F. Lu, X. Wang, D. Bi, Monoclonal antibody against
632 sulfaquinoxaline and quantitative analysis in chicken tissues by competitive indirect ELISA and lateral
633 flow immunoassay, Food Agric. Immunol. 22 (2011) 1–16.
634 https://doi.org/10.1080/09540105.2010.514895.
635 [47] N. Xu, L. Li, S. Song, L. Xu, H. Kuang, C. Xu, Development of a lateral flow immunoassay for the
636 detection of total malachite green residues in fish tissues, Food Agric. Immunol. 26 (2015) 870–879.
637 https://doi.org/10.1080/09540105.2015.1039498.
638 [48] D. Wild, Immunoassay for Beginners, in: Immunoass. Handb., Elsevier, 2013: pp. 7–10.
639 https://doi.org/10.1016/B978-0-08-097037-0.00002-6.
640 [49] A.M. D Quesada-González, D. Quesada-González, A. Merkoçi, Nanoparticle-based lateral flow
641 biosensors, Biosens. Bioelectron. 73 (2015) 47–63. https://doi.org/10.1016/J.BIOS.2015.05.050.
642 [50] Ł. Komsta, K. Wicha-Komsta, T. Kocki, Being Uncertain in Chromatographic Calibration—Some
643 Unobvious Details in Experimental Design, Mol. 2021, Vol. 26, Page 7035. 26 (2021) 7035.
644 https://doi.org/10.3390/MOLECULES26227035.
645 [51] D.B. Hibbert, Experimental design in chromatography: A tutorial review, J. Chromatogr. B. 910
646 (2012) 2–13. https://doi.org/10.1016/j.jchromb.2012.01.020.
647 [52] B. Dejaegher, Y. Vander Heyden, Experimental designs and their recent advances in set-up, data
648 interpretation, and analytical applications, J. Pharm. Biomed. Anal. 56 (2011) 141–158.
649 https://doi.org/10.1016/J.JPBA.2011.04.023.
650 [53] S. Cavalera, E. Alladio, E.A. Foglia, S. Grazioli, B. Colitti, S. Rosati, C. Nogarol, F. Di Nardo, T. Serra, V.

651 Testa, C. Baggiani, G. Maccabiani, E. Brocchi, L. Anfossi, Experimental design for the development of
652 a multiplex antigen lateral flow immunoassay detecting the Southern African Territory (SAT)
653 serotypes of foot-and-mouth disease virus, Microchim. Acta. 191 (2024) 9.
654 https://doi.org/10.1007/s00604-023-06090-6.
655 [54] S. Cavalera, G. Pezzoni, S. Grazioli, E. Brocchi, S. Baselli, D. Lelli, B. Colitti, T. Serra, F. Di Nardo, M.
656 Chiarello, V. Testa, S. Rosati, C. Baggiani, L. Anfossi, Investigation of the "Antigen Hook Effect" in
657 Lateral Flow Sandwich Immunoassay: The Case of Lumpy Skin Disease Virus Detection, Biosensors.
658 12 (2022) 739. https://doi.org/10.3390/bios12090739.
659 [55] S. Cavalera, B. Colitti, G.M. De Mia, F. Feliziani, S.D. Giudici, P.P. Angioi, F. D'Errico, D. Scalas, A.
660 Scollo, T. Serra, M. Chiarello, V. Testa, F. Di Nardo, C. Baggiani, A. Oggiano, S. Rosati, L. Anfossi,
661 Development of molecular and antigenic-based rapid tests for the identification of African swine
662 fever virus in different tissues, Talanta. 258 (2023) 124443.
663 https://doi.org/10.1016/j.talanta.2023.124443.
664 [56] A. Apilux, S. Rengpipat, W. Suwanjang, O. Chailapakul, Paper-based immunosensor with competitive
665 assay for cortisol detection, J. Pharm. Biomed. Anal. 178 (2020) 112925.
666 https://doi.org/10.1016/j.jpba.2019.112925.
667 [57] R. Matsuda, E. Rodriguez, D. Suresh, D.S. Hage, Chromatographic immunoassays: strategies and
668 recent developments in the analysis of drugs and biological agents, Bioanalysis. 7 (2015) 2947–2966.
669 https://doi.org/10.4155/bio.15.206.
670 [58] S.Y. Lu, C. Lin, Y.S. Li, Y. Zhou, X.M. Meng, S.Y. Yu, Z.H. Li, L. Li, H.L. Ren, Z.S. Liu, A screening lateral
671 flow immunochromatographic assay for on-site detection of okadaic acid in shellfish products, Anal.
672 Biochem. 422 (2012) 59–65. https://doi.org/10.1016/J.AB.2011.12.039.
673 [59] S. Yu, L. He, F. Yu, L. Liu, C. Qu, L. Qu, J. Liu, Y. Wu, Y. Wu, A lateral flow assay for simultaneous
674 detection of Deoxynivalenol, Fumonisin B1 and Aflatoxin B1, Toxicon. 156 (2018) 23–27.
675 https://doi.org/10.1016/J.TOXICON.2018.10.305.
676 [60] J. He, Practical Guide to ELISA Development, Immunoass. Handb. Theory Appl. Ligand Bind. ELISA
677 Relat. Tech. (2013) 381–393. https://doi.org/10.1016/B978-0-08-097037-0.00025-7.
678 [61] A. Abad, J.J. Manclús, F. Mojarrad, J. V. Mercader, M.A. Miranda, J. Primo, V. Guardiola, A. Montoya,
679 Hapten Synthesis and Production of Monoclonal Antibodies to DDT and Related Compounds, J.
680 Agric. Food Chem. 45 (1997) 3694–3702. https://doi.org/10.1021/JF9704219.
681 [62] F. Di Nardo, S. Cavalera, C. Baggiani, C. Giovannoli, L. Anfossi, Direct vs Mediated Coupling of
682 Antibodies to Gold Nanoparticles: The Case of Salivary Cortisol Detection by Lateral Flow
683 Immunoassay, ACS Appl. Mater. Interfaces. 11 (2019) 32758–32768.
684 https://doi.org/10.1021/acsami.9b11559.
685 [63] W.J. Inder, G. Dimeski, A. Russell, Measurement of salivary cortisol in 2012 – laboratory techniques

and clinical indications, Clin. Endocrinol. (Oxf). 77 (2012) 645–651. https://doi.org/10.1111/J.1365-2265.2012.04508.X.

[64] D.A. Papanicolaou, N. Mullen, I. Kyrou, L.K. Nieman, National Institute of Child Health and Human Development, Natl. Institutes Heal. 87 (2002) 4515–4521. https://doi.org/10.1210/jc.2002-020534.

[65] H. Raff, Utility of Salivary Cortisol Measurements in Cushing's Syndrome and Adrenal Insufficiency, J. Clin. Endocrinol. Metab. 94 (2009) 3647–3655. https://doi.org/10.1210/JC.2009-1166.

[66] M. Trilck, J. Flitsch, D.K. Lüdecke, R. Jung, S. Petersenn, Salivary cortisol measurement - A reliable method for the diagnosis of Cushing's syndrome, Exp. Clin. Endocrinol. Diabetes. 113 (2005) 225–230. https://doi.org/10.1055/S-2005-837667/ID/22/BIB.

[67] C.A. Carrasco, J. Coste, L. Guignat, L. Groussin, M.A. Dugué, S. Gaillard, X. Bertagna, J. Bertherat, Midnight Salivary Cortisol Determination for Assessing the Outcome of Transsphenoidal Surgery in Cushing's Disease, J. Clin. Endocrinol. Metab. 93 (2008) 4728–4734. https://doi.org/10.1210/jc.2008-1171.

[68] H. Raff, Salivary cortisol: A useful measurement in the diagnosis of Cushing's syndrome and the evaluation of the hypothalamic-pituitary-adrenal axis, Endocrinologist. 10 (2000) 9–17. https://doi.org/10.1097/00019616-200010010-00004.

[69] T. Carroll, H. Raff, J.W. Findling, Late-night salivary cortisol measurement in the diagnosis of Cushing's syndrome, Nat. Clin. Pract. Endocrinol. Metab. 2008 46. 4 (2008) 344–350. https://doi.org/10.1038/ncpendmet0837.

[70] W. Kedzierski, K. Strzelec, A. Cywińska, S. Kowalik, Salivary Cortisol Concentration in Exercised Thoroughbred Horses, J. Equine Vet. Sci. 33 (2013) 1106–1109. https://doi.org/10.1016/J.JEVS.2013.04.011.

[71] J.P. Hekman, A.Z. Karas, N.A. Dreschel, Salivary cortisol concentrations and behavior in a population of healthy dogs hospitalized for elective procedures, Appl. Anim. Behav. Sci. 141 (2012) 149–157. https://doi.org/10.1016/J.APPLANIM.2012.08.007.

[72] A. Riek, L. Schrader, F. Zerbe, S. Petow, Comparison of cortisol concentrations in plasma and saliva in dairy cattle following ACTH stimulation, J. Dairy Res. 86 (2019) 406–409. https://doi.org/10.1017/S0022029919000669.

[73] G. Chacón Pérez, S. García-Belenguer Laita, J.C. Illera del Portal, J. Palacio Liesa, Validation of an EIA [enzyme immunoassay] technique for the determination of salivary cortisol in cattle, Spanish J. Agric. Res. 2 (2004) 45. https://doi.org/10.5424/sjar/2004021-59.

[74] J.J. Roe, C. Ward Thompson, P.A. Aspinall, M.J. Brewer, E.I. Duff, D. Miller, R. Mitchell, A. Clow, Green Space and Stress: Evidence from Cortisol Measures in Deprived Urban Communities, Int. J. Environ. Res. Public Health. 10 (2013) 4086–4103. https://doi.org/10.3390/IJERPH10094086.

[75] X. Pan, Z. Wang, X. Wu, S.W. Wen, A. Liu, Salivary cortisol in post-traumatic stress disorder: A

systematic review and meta-analysis, BMC Psychiatry. 18 (2018) 1–10. https://doi.org/10.1186/S12888-018-1910-9/TABLES/3.

[76] A.R. Tarullo, A.M. St. John, J.S. Meyer, Chronic stress in the mother-infant dyad: Maternal hair cortisol, infant salivary cortisol and interactional synchrony, Infant Behav. Dev. 47 (2017) 92–102. https://doi.org/10.1016/J.INFBEH.2017.03.007.

[77] K.F.S. Petrelluzzi, M.C. Garcia, C.A. Petta, D.M. Grassi-Kassisse, R.C. Spadari-Bratfisch, Salivary cortisol concentrations, stress and quality of life in women with endometriosis and chronic pelvic pain, Stress. 11 (2008) 390–397. https://doi.org/10.1080/10253890701840610.

[78] D. Pfefferle, S. Plümer, L. Burchardt, S. Treue, A. Gail, Assessment of stress responses in rhesus macaques (Macaca mulatta) to daily routine procedures in system neuroscience based on salivary cortisol concentrations, PLoS One. 13 (2018) e0190190. https://doi.org/10.1371/journal.pone.0190190.

[79] E. Fries, J. Hesse, J. Hellhammer, D.H. Hellhammer, A new view on hypocortisolism, Psychoneuroendocrinology. 30 (2005) 1010–1016. https://doi.org/10.1016/j.psyneuen.2005.04.006.

[80] T. Yonekura, K. Takeda, V. Shetty, M. Yamaguchi, Relationship between salivary cortisol and depression in adolescent survivors of a major natural disaster, J. Physiol. Sci. 64 (2014) 261–267. https://doi.org/10.1007/s12576-014-0315-x.

[81] S. Chojnowska, I. Ptaszynska, P. Ptaszynska-Sarosiek, A. K¸ Epka, M.K. Knas, N. Waszkiewicz, Clinical Medicine Salivary Biomarkers of Stress, Anxiety and Depression, J. Clin. Med. 10 (2021) 517. https://doi.org/10.3390/jcm.

[82] Z. Wang, Y. Zhu, S. Ding, F. He, R.C. Beier, J. Li, H. Jiang, C. Feng, Y. Wan, S. Zhang, Z. Kai, X. Yang, J. Shen, Development of a Monoclonal Antibody-Based Broad-Specificity ELISA for Fluoroquinolone Antibiotics in Foods and Molecular Modeling Studies of Cross-Reactive Compounds, Anal. Chem. 79 (2007) 4471–4483. https://doi.org/10.1021/ac070064t.